ARTICLE IN PRESS

Available online at www.sciencedirect.com

ScienceDirect

Biomaterials ▮ (▮▮▮▮) ▮▮▮–▮▮▮

Biomaterials

www.elsevier.com/locate/biomaterials

Permanent, non-leaching antibacterial surfaces—2: How high density cationic surfaces kill bacterial cells

Hironobu Murata[a], Richard R. Koepsel[b,c], Krzysztof Matyjaszewski[c,d], Alan J. Russell[a,b,c,*]

[a]*Department of Bioengineering, University of Pittsburgh, Pittsburgh, PA 15260, USA*
[b]*Department of Chemical and Petroleum Engineering, University of Pittsburgh, PA 15260, USA*
[c]*Department of Surgery, McGowan Institute for Regenerative Medicine, University of Pittsburgh, Suite 200, 100 Technology Drive, Pittsburgh, PA 15219, USA*
[d]*Center for Macromolecular Engineering, Department of Chemistry, Carnegie Mellon University, 4400 Fifth Avenue, Pittsburgh, PA 15213, USA*

Received 26 April 2007; accepted 7 June 2007

Abstract

Rational controlled synthesis of poly(quaternary ammonium) compounds has been used to prepare antimicrobial polymer brushes on inorganic surfaces. The systematic variation of several structural parameters of the polymeric brushes allowed us to elicit the minimum surface requirements and a probable mechanism of action for *Escherichia coli* cell kill. Polymeric brushes were prepared by surface-initiated atom transfer radical polymerization of 2-(dimethylamino)ethyl methacrylate (DMAEMA), a method that allows the molecular weight of the polymer chains to be precisely controlled as they grow from the target surface. The tertiary amino groups of the polyDMAEMA were then quaternized with alkyl bromides to provide a surface with antimicrobial activity. Dry layer thickness of the polymer brushes was controlled by polymerization time and/or initiator density on the surface. This tunability of surface structure allows the antimicrobial polymer brushes to be tailored rationally. A combinatorial screening tool was developed to elucidate the role of chain length and chain density on cell kill in a single experiment. The results indicate that surface charge density, is a critical element in designing a surface for maximum kill efficiency. The most biocidal surfaces had charge densities of greater than $1–5 \times 10^{15}$ accessible quaternary amine units/cm^2. The relevance of this finding to the mechanism of action is discussed.

Keywords: Antibacterial; Bacteria; PolyDMAEMA; Surface modification; Atom transfer radical polymerization

1. Introduction

Antimicrobial materials are used to prevent microbial infection in a wide variety of industrial, medical, community, and private settings. To obtain biocidal effect without releasing biocide into the environment, antimicrobial species can be irreversibly (covalently) coupled to material surfaces. Such materials also reduce the likelihood of generating resistance to the active agent. Recent studies have reported the successful covalent attachment of polymeric antimicrobial materials onto glass, [1–4] polymer, [5–12] paper, [4] and metal [13]. In many of these cases the biocidal polymer [14,15] contained cationic groups, such as alkyl pyridinium [1–3,5–8] or quaternary ammonium [4,9–13]. Cationic antimicrobials are especially well positioned to play a role in the development of self-disinfecting surfaces [16]. Recently, quaternized poly-2-(dimethylamino)ethyl methacrylate (polyDMAEMA) has been used as a cationic surfactant [17], within polymer microspheres, [18] in which they exhibit high levels of antibacterial activity.

The quaternary ammonium salts (QAS) are among the most commonly used of the cationic antimicrobials [16]. Within the large group of QAS, the polymeric quaternary amines show perhaps the greatest promise in the realm of surface-active compounds. Several reports have suggested that the mechanism of action of polycations involves disruption of the integrity of the

*Corresponding author. Department of Bioengineering, University of Pittsburgh, Pittsburgh, PA 15260, USA.
E-mail address: arussell@pitt.edu (A.J. Russell).

0142-9612/$ - see front matter © 2007 Elsevier Ltd. All rights reserved.
doi:10.1016/j.biomaterials.2007.06.012

cell membrane [1,3,6–10]. Two mechanistic hypotheses have been put forward to explain why a wide range of species are susceptible to polyquaternary amine-induced death. The most quoted theory hypothesizes that long cationic polymers penetrate cells and thereby disrupt the membrane, like a needle bursting a balloon [1,3,6,12]. This concept has persisted in the literature for some time [14,15] despite the fact that in one of the first demonstrations of a permanent antimicrobial surface, a monolayer of 3-(trimethoxysilyl)-propyldimethyloctadecyl ammonium chloride bound to a surface, was known to be highly antimicrobial [19]. The mechanistically-driven design of even more effective surface active QAS-based antimicrobials naturally depends on whether this hypothesis fully explains the observation that all polymeric QAS can kill microbes, from viruses to fungi, even though the different microbes have dramatically different membrane properties and dimensions. An alternative mechanism that has been offered to explain the breadth of bioactivity posits that a highly charged surface can induce what is essentially an ion exchange between the positive charges on the surface and structurally critical mobile cations within the membrane [2]. Upon approaching a cationic surface, the structurally essential divalent cations of the membrane are relieved of their role in charge neutralization of the membrane components and are thus free to diffuse out of the membrane. The loss of these structural cations results in a loss of membrane integrity [2].

While soluble compounds may be able to penetrate the cell envelope, surface-bound molecules are constrained by their molecular length and could only penetrate the cell membrane if they extended far enough away from the surface. Most bacteria have non-deformable, rigid outer envelopes. For the Gram negative *Escherichia coli*, the thickness of the cell envelope (cytoplasmic membrane, periplasmic space, peptidoglycan, and outer membrane from inside to outside) has recently been shown to be 46 nm [20–22]. The measurement is about 45–55 nm for the Gram positive *Bacillus subtilis* [20] which lacks an outer membrane but has a thicker peptidoglycan layer. This would mean that the wet layer thickness of a polymer coating on a surface should be at least 75 nm in order to effectively penetrate the cytoplasmic membrane and kill the cells. QAS polymers have recently been shown to kill fungal mycelia which have cell walls wider than 80 nm [23]. We have begun to explore how high density polymer brushes exhibit such broad bioactivity. Some of the highest density polymer brushes can be formed by surface-initiated atom transfer radical polymerization (ATRP) [4], which is among the most efficient controlled/"living" radical polymerization systems [24–31]. ATRP-synthesized covalently attached polymer brushes also yield precise molecular weights and/or grafting density. We show herein that short chains with high grafting density and long chains with low grafting density are equally effective against *E. coli*.

2. Materials and methods

N,*N*-dimethylaminoethyl methacrylate (DMAEMA), bromoethane, 1,1,4,7,10,10-hexamethyltriethylenetetramine (HMTETA), copper (I) bromide (CuBr), 2-bromo-2-methylpropionic acid bromide, allylamine, allyl alcohol, acetone, acetonitrile, chloroform, methanol and *N*,*N*-dimethylformamide (DMF) were purchased from Sigma-Aldrich Chemical Co. Pre-cleaned glass slides were purchased from Corning and Fisher. The substrates for transmission FTIR spectroscopy and ellipsometry were polished silicon wafers (Silicon Quest International, California) with a natural SiO_2 layer of approximately 2–3 nm. The glass slides and silicon wafers were treated with "piranha" solution (H_2SO_4:H_2O_2, 4:1) for 1 h. After treatment the substrates were rinsed with de-ionized water and dried under stream of air.

2.1. Measurement

^{1}H NMR spectra were recorded on a Bruker Avance (300 MHz) spectrometer (Center for molecular analysis, Carnegie Mellon University) in DMSO-D_6 and $CDCl_3$. Routine FT-IR spectra were obtained with an ATI Mattson Infinity series FTIR spectrometer (Center for molecular analysis, Carnegie Mellon University). UV–vis spectra were recorded on a Perkin-Elmer Lambda 2. Contact angles were obtained with a VCA Optima (AST products, Inc.) with a drop size 1.50 μL of de-ionized water. The layer thicknesses of the grafted polymers were obtained by a discrete wavelength ellipsometer PhE-101 (Micro Photonics Inc.) with a He–Ne laser ($\lambda = 632.8$ nm) at a 70° incidence angle. The refractive index of the polymer brushes on the substrates was assumed to be $n = 1.50$. The data were collected at multiple spots on each wafer.

2.2. Synthesis of covalently attached quaternary ammonium polymer brushes on substrates

2.2.1. Synthesis of 3-(2-bromoisobutyroyl)-aminopropyltrimethoxysilane

A solution of allylamine (7.5 mL, 100 mmol), triethylamine (21 mL, 150 mmol) and dichloromethane (200 mL) was slowly mixed with a solution of 2-bromo-2-methylproionic acid bromide (13.6 mL, 110 mmol) in dichloromethane (50 mL) at 0 °C. The mixture was then stirred for 4 h at room temperature. The reaction mixture was washed sequentially with water, a saturated aqueous solution of $NaHCO_3$, 0.5 M HCl, and a saturated aqueous solution of NaCl. The organic layer was dried over anhydrous $MgSO_4$, filtered, and concentrated by rotary evaporation. A solution of the resultant allylic compound (5 mL, 24.2 mmol) and toluene (20 mL) was mixed with trimethoxysilane (7.7 mL, 60.5 mmol) and Pt/C (10% Pt, 100 mg), then the mixture was stirred at 60 °C overnight. Toluene and excess trimethoxysilane were removed by evaporation in vacuo. The crude residue was used for initiator immobilization after the Pt/C was filtered away. ^{1}H NMR (300 MHz, $CDCl_3$) δ 0.73 (t, 2H, $J = 8.4$ Hz, $SiCH_2CH_2CH_2$), 1.61–1.72 (m, 2H, $SiCH_2CH_2CH_2NH$), 1.96 (s, 6H, $NHCOCBr(CH_3)_2$), 3.23–3.31 (m, 2H, $CH_2CH_2CH_2NH$), 3.59 (s, 9H, $Si(OCH_3)_3$), 6.89 (broad s, 1H, amide).

2.2.2. Synthesis of 3-(2-bromoisobutyryl)-propyltrimethoxysilane

The title compound was synthesized from allyl alcohol instead of allylamine in a similar manner as 3-(2-bromoisobutyroyl)-aminopropyltrimethoxysilane. ^{1}H NMR (300 MHz, $CDCl_3$) δ 0.73 (t, 2H, $J = 8.4$ Hz, $SiCH_2CH_2CH_2$), 1.73–1.84 (m, 2H, $SiCH_2CH_2CH_2OCO$), 1.95 (s, 6H, $OCOCBr(CH_3)_2$), 3.59 (s, 9H, $Si(OCH_3)_3$), 4.17 (t, $J = 6.5$ Hz, 2H, $SiCH_2CH_2CH_2OCO$).

2.2.3. Initiator immobilization of on planar glass

Planar glass slides and silicon wafers were placed into initiator solutions of either 3-(2-bromoisobutyroyl)-animopropyltrimethoxysilane or 3-(2-bromoisobutyryl)-propyltrimethoxysilane and trimethoxypropylsilane at various designated molar ratios with triethylamine (0.1% v/v) and toluene (100 mL) at 80 °C for 1 h. The treated slides were removed

Please cite this article as: Murata H, et al. Permanent, non-leaching antibacterial surfaces—2: How high density cationic surfaces kill bacterial.... Biomaterials (2007), doi:10.1016/j.biomaterials.2007.06.012

from the reaction, rinsed with toluene, methanol and acetone, and then dried in a nitrogen stream.

2.2.4. "Surface-initiated" ATRP of DMAEMA on the substrate

A monomer solution was created by combining DMAEMA (8.4 mL), HMTETA (68 μL) and acetone (50 mL). The solution was then degassed using five freeze-pump-thaw cycles, then adding Cu(I)Br (36 mg) and conducting five cycles of vacuum purging and backfilling with nitrogen. The initiator-modified slides and silicon wafers were placed in a polymerization tube and put through five cycles of vacuum purging and backfilling with nitrogen. These substrates were then covered with the degassed monomer solution and heated to 40 °C for targeted times. The substrates, now with polymer brushes, were then extracted in acetone using a shaker for at least 6 h to remove free polymer from the layer. Finally these substrates were rinsed with methanol and then acetone.

2.2.5. Quaternization of polyDMAEMA brushs with alkyl bromide

The substrates with polymer brushes were placed in acetonitrile (50 mL), then 1-bromoethane (10 mL) was added and the substrates and solution were heated at 40 °C overnight. The substrates were extracted in deionized water, then rinsed in methanol and finally acetone.

2.2.6. Hydrolysis testing

Hydrolysis testing was performed using polyquaternary amine (PQA) brushes grown from amide or ester linkages in the self-assembled initiator on the silicon wafers. Loss of polymer from the surface was recorded as a decrease the layer thickness on the substrate. Samples were put in 0.3 mM of sodium phosphate buffer (pH 7.4) and shaken at 37 °C. Samples were removed at intervals, rinsed with deionized water, dried under a stream of nitrogen, and the layer thickness of the treated PQA brushes was measured by ellipsometry.

2.2.7. Generating a gradient of initiator on planar glass slides

Planar glass slides and silicon wafers ($5.0 \times 7.5\,mm^2$) were placed into a reaction vessel, and 50 mL of initiator solution in toluene (5.0 mM) was carefully poured into the bottom of the reactor at 80 °C for 15 min. Blocker solution (500 mM in toluene) was added using syringe pump at a flow rate of 1 mL/min. The reaction was kept at 80 °C for 1 h following which the treated slides were sequentially rinsed with toluene, methanol, then acetone and dried at 80 °C.

2.2.8. Gradient "surface-initiated" ATRP of DMAEMA on the slide

Monomer solution, DMAEMA (50.4 mL), HMTETA (408 μL) and acetone (300 mL), was degassed by five freeze-pump-thaw cycles. Cu(I)Br (216 mg) was added followed by five cycles of vacuum purging and backfill with nitrogen. Initiator modified slides and silicon wafers were placed in a polymerization tube and followed by a further five cycles of vacuum purging and backfill with nitrogen. The degassed monomer solution was slowly added into the polymerization vessel using syringe pump at a flow rate of 0.5 mL/min at 40 °C until the monomer solution reached the top of slides. The reaction was continued for an additional 1 h and the slides were then extracted in acetone for at least 6 h to remove free polymer from the layer then finally sequentially rinsed with methanol and acetone.

2.2.9. Determination of surface accessible quaternary amines

The density of quaternary ammonium groups on surfaces was measured as the amount of fluorescein bound per unit area. Polyquat modified surfaces ($1 \times 1\,cm^2$) were placed in a 15 mL test tube containing 10 mL of a 1 wt% solution of fluorescein (Sodium salt) in distilled water for 10 min. The fluorescein solution was decanted and the samples were extensively rinsed with distilled water then placed in 3 mL of 0.1% solution of cetyltrimethylammonium chloride in a fresh tube. The samples were shaken for 20 min at 300 rpm on an orbital shaker to desorb the dye. The absorbance of the resultant aqueous solution was measured at 501 nm after adding 10% v/v of 100 mM phosphate (pH 8.0). The amount of fluorescein bound to the PQA brush was calculated using a value of $77\,mM^{-1}\,cm^{-1}$ as the extinction coefficient [1]. The number of QA units on the brush was determined by using the fluorescein concentration assuming a 1:1 fluorescein to accessible QA ratio [1].

2.2.10. Antimicrobial activity determination

Antimicrobial testing of sectioned portions of the glass slides was performed using a modified ASTM standard: *E2149-01 Standard Test Method for Determining the Anti-microbial Activity of Immobilized Antimicrobial Agents Under Dynamic Contact Conditions* [44]. Details of the procedure have been reported [4]. Briefly, a colony of *E. coli* K12 grown on a Luria agar (L-agar) plate was used to inoculate 5 mL of Luria broth in a sterile 50 mL conical tube. The culture was incubated at 37 °C while being shaken at 300 rpm (G24 Environmental Incubator Shaker, New Brunswick Scientific) for 18–20 h. The cells were diluted with Sorensen's Phosphate Buffer (pH 6.8, 0.3 mM KH_2PO_4) to the desired concentration. The actual number of cells used for a given experiment was determined by standard serial dilution. The glass pieces with PQA brushes (typically $1 \times 2.5\,cm^2$, both sides treated to give $5\,cm^2$ of surface) were incubated with 5 mL of cell suspension in a 50 mL conical tube (Falcon) at 37 °C and 300 rpm. An untreated glass slide was used as a control. Samples were taken after 1 h, diluted appropriately, and plated on L-agar plates. Results are reported as the total number survivors and as the number of cells killed/unit surface area compared to an untreated blank sample.

2.3. Surface scans of gradient slides

Gradient slides were prepared as above. A 0.5 mL of an overnight culture of *E. coli* in LB medium was pelleted in a microfuge, the supernatant was pipetted off and the cells were suspended in 1 mL Sorensen's buffer. A 0.3 mL of the cell suspension (approximately 5×10^8 cells) was pipetted onto the surface of the slide and covered with another slide. After 30 min incubation at room temperature the cover slide was removed and non-adherent cells were removed by gently rinsing the gradient slide with 10 mL water. The adherent cells were immediately stained using a BacLite® live/dead staining kit (Invitrogen, Carlsbad, CA) prepared by diluting 3 μL of each of the kit components in 500 μL deionized water. A total of 200 μL of the dye suspension was pipetted onto the surface of the gradient slide, covered with a clean slide and incubated for 15 min at room temperature in the dark at which time the cover slide was removed, the gradient slide was gently rinsed with 10 mL deionized water and allowed to air dry. The dry stained slide was scanned in an iCyte laser scanning imaging cytometer (Compucyte, Cambridge MA). The iCyte measured fluorescence in the green and red wavelengths corresponding to the emission from green fluorescent dye, Syto 9, and the red fluorescent dye, propidium iodide, respectively. Syto 9 stains live cells and propidium iodide stains dead cells. The iCyte saves pictures of each microscopic field and generates a color composite image of the entire slide. Images from each detector are also saved facilitating analysis of the regions of the slide that bind cells, bind and kill cells or have no discernable activity. Composite images were further analyzed and surface plots generated with the Image J software package (http://rsb.info.nih.gov/ij/).

3. Results

3.1. Impact of polyquaternary ammonium chain length on efficacy of E. coli kill

In order to analyze carefully whether high density short chain surface-bound poly(quaternary ammonium) compounds (PQAs) could kill bacteria, we modified our previous synthetic technique [4] to guarantee that leaching of the polymers from the surface would not be possible over the time course of our experiments. Initiators were synthesized by reacting 2-bromo-2-methylpropionic acid

Please cite this article as: Murata H, et al. Permanent, non-leaching antibacterial surfaces—2: How high density cationic surfaces kill bacterial.... Biomaterials (2007), doi:10.1016/j.biomaterials.2007.06.012

bromide with allylamine or allyl alcohol, followed by hydrosilation with trimethoxysilane in the presence of a platinum catalyst (see Scheme s1 in Supplementary Information), self-assembled on the glass or silicon wafer surfaces, and used as sites for polymerization with 2-(dimethylamino)ethyl methacrylate (DMAEMA) (Scheme s2 in Supplementary Information). The polyDMAEMA brushes were quaternized with bromoethane and the results verified with transmittance FTIR (Figure s1 in Supplementary Information). The resulting amide-bound PQA brushes were stable on the surface of glass for many days (see supplemental figure s2 in Supplementary Information).

The chain length of polymers synthesized by ATRP as a function of reaction time for surface-initiated reactions at constant initiator density has been studied in depth [25,30–35]. As shown in Fig. 1, the layer thickness of polyDMAEMA (filled circles) brushes increases steadily with reaction time until about 10 h. Such a loss of linearity has previously been linked to the loss of active chain ends or a reduced rate of monomer diffusion [32].

Once quaternized, the dry layer thicknesses of the PQA polymer brushes increased 1.3–1.7 fold compared to the original layer thicknesses of the polyDMAEMA brushes (see closed triangles in Fig. 1). Dry layer thickness (L) is related to molecular weight (M_w), grafting density and polymer density. In this experiment the molar mass of the repeat units of the PQA brush ($M_w = 266.2$ g/mol) is approximately 1.7 times larger than that of the polyDMAEMA brush ($M_w = 157.2$ g/mol). The change in layer thickness is also of the same magnitude. Given our interest in determining the efficacy of surface-bound PQAs in killing bacterial cells, it was important to determine what fraction of cationic groups were accessible to a bacterial membrane. Equations exist that incorporate terms for graft density of the polymer chains and the polymer density to calculate the number of repeat units from dry layer thickness. Unfortunately, however, the many assumptions used in developing these equations reduce the attractiveness of calculating the number of accessible cationic groups from dry layer thickness. In order to directly measure the accessible QA units we exploited the observation that fluorescein binds tightly to quaternary ammonium groups [36]. Indeed, this binding has previously been used to calculate the concentration of solvent accessible QA units on surfaces [1,2,7].

In order to quantify the relationship between chain length, charge availability, density of polymer and cell kill activity we modified highly ordered surfaces (silicon wafers) and optically transparent surfaces (glass). The silicon wafers were necessary for ellipsometric measurements of the layer thickness (Fig. 1) and the glass samples were required for optical microscopy. Fluorescein staining of both the silicon and glass surfaces (Fig. 2) showed that the solvent accessible surface charge density was the same on both glass and silicon surfaces when these surfaces were co-produced in a single reactor. This implied, assuming equal polymer densities, that the polymer molecular weight on each surface was the same. Critically, this experiment demonstrated that data collected from silicon wafers that are co-produced with glass slides could be used to predict the dry layer thickness on the glass slide.

Next, we took these surfaces and determined the antimicrobial capacity of surface-bound PQAs on silicon (Table 1). The number of viable *E. coli* cells in a suspension was determined before and after incubation with the surface as described previously [4]. The data in Table 1 report the results for sets of silicon wafers that were

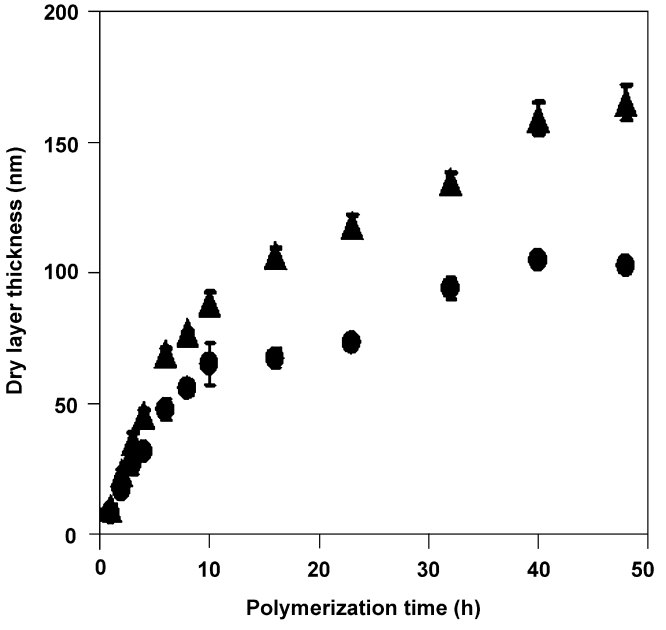

Fig. 1. Dry layer thickness of high density polyDMAEMA brushes on silicon wafers as a function of polymerization time before (●) and after quaternization with bromoethane (▲).

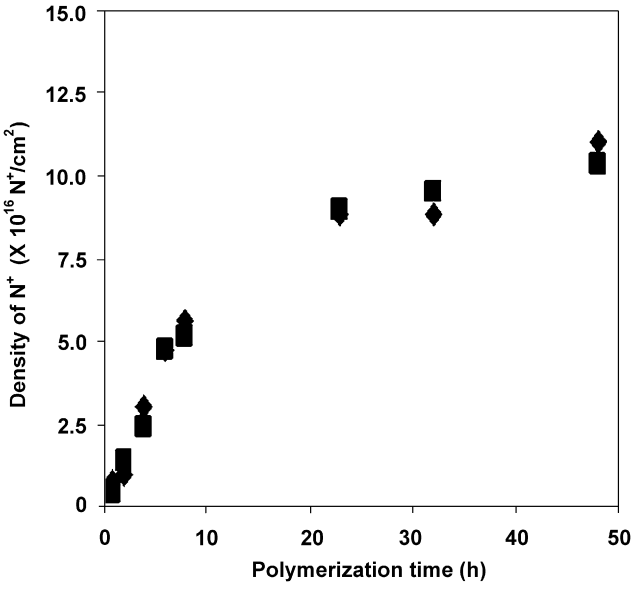

Fig. 2. Experimentally derived available surface charge density of high density polymer brushes synthesized by ATRP on glass (◆) and silicon wafers (■).

Please cite this article as: Murata H, et al. Permanent, non-leaching antibacterial surfaces—2: How high density cationic surfaces kill bacterial.... Biomaterials (2007), doi:10.1016/j.biomaterials.2007.06.012

Table 1
The effect of polymerization time on surface charge density and antimicrobial activity of PQA brushes on silicon wafers

Polymerization time (h)[a]	Dry layer thickness (nm)[b]	Solvent accessible surface charge/cm^2	Number of *E. coli* cells killed/cm^2 [c]
1	5.1	4.68×10^{14}	4.7×10^4
2	19.1	1.40×10^{15}	1.0×10^4
4	36	2.45×10^{15}	1.0×10^5
6	51.5	4.78×10^{15}	1.6×10^5
8	55.5	5.13×10^{15}	$>2.0 \times 10^5$
10	88.8	5.77×10^{15}	$>2.0 \times 10^5$
16	106.9	7.95×10^{15}	$>2.0 \times 10^5$
23	109.5	8.93×10^{15}	$>2.0 \times 10^5$
32	99.7	9.51×10^{15}	$>2.0 \times 10^5$
48	123.3	1.03×10^{16}	$>2.0 \times 10^5$

[a]The surface used is covered with 100% of initiator-TMS.
[b]Dry layer thickness was estimated by ellipsometry for the silicon wafer samples.
[c]Surfaces were incubated with 2.0×10^5 *E. coli*/cm^2 surface.

covered with a monolayer of initiator, subjected to polymerization for various times, and quaternized with bromoethane. The results did not conform with our expectation that powerful biocidal surfaces would be generated only at long polymerization times. Surfaces with dry layer brush thicknesses as small as 10 nm killed cells. A 10 nm layer thickness approximates to a molecular weight of polymer on the order to 15–20,000. If one assumes, as others have shown, [33,35] that our surface-initiated polymer synthesis results in a polymer with polydispersity index (PDI = M_w/M_n) of at most 1.5, then as chain length increases from $M_w = 15{,}200$ to 28,800 the fraction of chains which exceed an M_w of 75,000 (the length of chain that has been postulated to penetrate a cell) can be calculated to increase smoothly from 0 to 0.83%. A dense, low polydispersity polymer brush with a dry layer thickness of 10 nm cannot extend through an *E. coli* cell envelope. The cell kill efficiency of these PQA surfaces increases by 10–20 fold when dry layer thickness exceeds 20 nm on the silicon samples. Above 55 nm the kill capacity exceeds the number of cells in the challenge and thus the upper limit of the capacity cannot be adequately determined.

The brush layer thickness at which there is a significant increase in bacterial kill capacity is less than the width of the *E. coli* cell membrane. It was also surprising to us that while a 36 nm dry layer thickness could kill cells with high efficiency, surfaces with 19 nm dry layer thicknesses had considerably less kill capacity. Neither surface contains significant fractions of molecules long enough to penetrate cells.

3.2. Effect of PQA chain density on efficacy of E. coli kill

The density of polymers grown from a surface has been tuned rationally by controlling the initial initiator concentration on the substrate [25,35–41]. In a variation of this process, Jones et al. [34] reported controlling the polymer density of ATRP-synthesized brushes by varying the concentration of the initiator molecules in self-assembled monolayers. In our study, the grafting density of polymer brushes was varied by using a solution of to which trimethoxypropylsilane was added to block sites on the surface that would otherwise be occupied by the initiator. The dry layer thickness of polyDMAEMA brushes grown on series of silicon wafers with varying initiator densities is shown in Fig. 3. The thickness of the layer increases with increasing density until the initiator density is about 10% at which point there is very little additional increase in the layer thickness. This is likely due to steric hindrance at the initiation of chain growth and implies that only about 10% of the possible initiation sites are being utilized even when all of the potential initiator binding sites are occupied. As seen in Fig. 1, when the polyDMAEMA brushes were quaternized with bromoethane, the layer thickness increases in proportion to the additional mass added through the quaternization reaction.

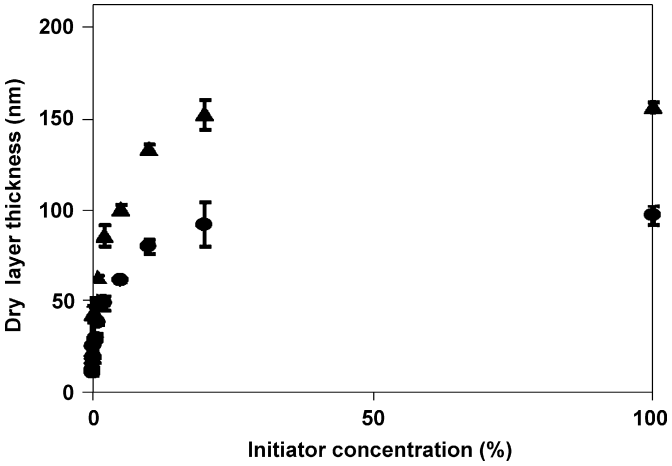

Fig. 3. Dry layer thickness of polyDMAEMA brush as function of initiator concentration before (●) after (▲) quaternization with bromoethane.

In order to explore further the high density, short chain-induced cell kill, we studied the solvent accessible surface charge density of a series of surfaces with varying initiator densities followed by a fixed 4 h polymerization time (Table 2). The experimentally determined solvent accessible

Table 2
Impact of initiator concentration on solvent accessible surface charge density and antimicrobial activity[a]

Initiator concentration (%)	Charge/unit area[b] ($\times 10^{15}$ N^+/cm^2)	Antimicrobial activity[c] (Kill/cm^2)
0	0	0
0.01	0.65	1.3×10^5
0.1	0.75	2.5×10^5
1	1.08	$>3.4 \times 10^5$
10	1.18	$>3.4 \times 10^5$
100	3.05	$>3.4 \times 10^5$

[a]Polymerization time in all cases was fixed at 4 h.
[b]Estimated by fluorescein staining test.
[c]Samples were challenged with 3.4×10^5 *E. coli*/cm^2.

surface charge increased from 0.65 to 3.05×10^{15} charges/cm^2 with increasing brush density. The impact of the change in surface charge density on cell kill efficacy for these short brushes is revealing in that it shows that the cell kill efficacy increases as the charge density increases. As in the experiment where we controlled chain length by changing polymerization time, complete kill of the bacterial challenge was dependent on a solvent accessible surface charge density in excess of 1×10^{15} charges/cm^2. Importantly in this experiment, in which all samples were polymerized for an identical time and are therefore expected to be the same size, the increase in cell kill was independent of the variations in molecular weight Although the experimentally determined solvent accessible surface charge density was high enough to kill, it is important to stress that the dry layer thickness of these surfaces was between only 4.4 and 8.0 nm (based on measurement of a co-produced silicon wafer). On these surfaces, cell death did not require the polymer to penetrate the cell membrane. When combined with the observation that cell kill increases with increasing polymerization time which is reflected in a concomitant increase in surface charge we see that two independent variants in surface polymer synthesis arrive at similar results with respect to the dependence of cell kill on surface charge density.

3.3. Upper limit of cell kill

Since cell kill increases as a function of surface charge density, we were interested in exploring the biocidal capacity of a highly charged surface. A set of glass slides were initiated using a 100% initiator solution and then polymerized for 20 h in order to maximize both polymer density and layer thickness. The available surface charge density of the slides was measured as 8×10^{15} charges/cm^2. We challenged these surfaces with increasing numbers of cells (Fig. 4) and demonstrated that the maximum kill capacity for this surface charge was almost 10^8 cells/cm^2. This is an interesting number because an average *E. coli* cell has dimensions of 0.5×2.0 μm and each cell should cover about 1 μm^2 of the surface. A 1 cm^2 surface should therefore be completely covered with 1×10^8 cells if they were perfectly arrayed. In Fig. 4 the drop off in the percent

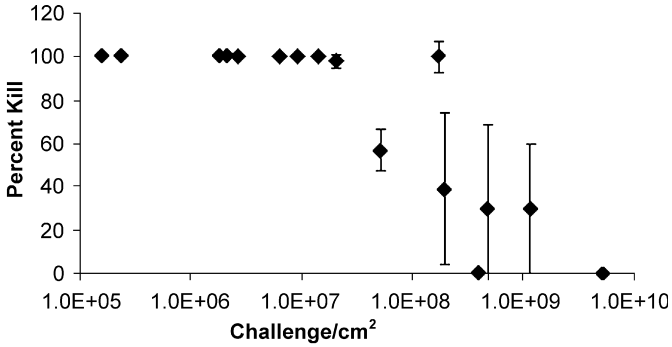

Fig. 4. Determination of the cell kill capacity for a high density surface. Samples of a glass surface with 8×10^{15} charges/cm^2 were incubated with increasing challenges of *E. coli*. The survivors were counted and compared with blank samples similarly challenged. The % of the challenge cells killed is plotted against the challenge concentration.

kill with increasing challenge occurs at around 10^8 cells/cm^2 surface. The assay, in which the surface is shaken with a suspension of cells, is designed so that all cells in the suspension should see the surface during the one hour time of the assay. The cells bind tightly to the surface but can potentially be displaced by the shear forces experienced by the surface during the assay. As the number of cells reaches or exceeds the number that would saturate the surface the probability of an individual cell interacting with an unoccupied space on the surface is reduced and some cells escape being killed. Further, in previous work [4] we demonstrated that the disruption of the cell membrane results in the internal contents of the cell becoming bound to the PQA surface. It is likely that this cell residue is fouling the surface even in this assay. Still, these results show that a surface with very high surface charge density can kill the equivalent of almost a monolayer of bacteria and likely more if the fouling materials can be removed.

3.4. Combinatorial analysis of effect of PQA chain length and density on cell kill efficacy

ATRP is uniquely capable of generating very dense short and/or long polymer brushes that appear to be able to kill cells without penetrating the membrane. We decided, therefore, to explore the minimum surface requirements

for cell kill. Because we use chemistry to control the growth of the polymers from the surface we have a tool through which we can develop a surface of tightly defined but varying properties. We established the synthetic tools necessary to generate smooth continuous gradients of length and density on a single glass slide or silicon wafer. The successful synthesis of such a modified glass construct (and the equivalent silicon wafer construct) allowed us to simultaneously visualize how bacterial cells behave as a function of location on the glass. This type of combinatorial screening of biocidal polymers on surfaces has not been reported previously.

The combinatorial screening surface was generated in a relatively simple reactor that exposed a surface to gradually decreasing initiator concentration. At the beginning of the experiment the reactor contained a 0.5 mM solution of initiator. The total amount of the initiator was such that it covered the bottom 1 cm of the slide. Concentrated blocker solution (500 mM) was added at a constant rate over the course of 5 h. The effect of this process is to generate a logarithmic gradient of initiator with 100% of the available sites bound to initiator at one end and 0.1% of the sites occupied at the other end (see supplemental information for detailed description of the gradient protocol). The results in Fig. 3 above showed that the polymer growth reached a maximum at around 20% initiator. Use of an exponential gradient thus expanded the area of the slide where the majority of change occurred.

The slides containing the gradient in initiator concentration were then rotated through 90° and the reactor was then used to grow polymer from those initiation points. Because the reactor was filled gradually during synthesis, the chain length at any given point was changed predictably and smoothly. The principle of two-dimensional (2-D) gradient surfaces is described in greater detail elsewhere [38,42].

The 2-D gradients of PQA chain length and density that we synthesized on silicon wafers were analyzed by ellipsometry and fluorescein staining to measure the dry layer thickness and the solvent accessible surface charge density as a function of position on the slide (Fig. 5). The dry layer thickness increased as a function of both incubation time and initiator concentration. Since surface hydrophobicity is a function of length, architecture, and density, we also determined the contact angle at each point on the surface the results fitting our expectations (supplemental figure s3).

A glass slide with a 2-D gradient of polymer, produced simultaneously in the same reactor as the silicon wafer described above, was assayed for its ability to bind and kill *E. coli*. The 2-D gradient surfaces allow us to simultaneously determine the minimum effective degree of modification as polymer density and polymer length required to derive effective biocidal surfaces. The entire slide was incubated with *E. coli* by dropping a suspension of bacteria onto the slide and then covering the slide with a plain unmodified slide to evenly spread a thin layer of cells across the surface. After fifteen minutes, non-adherent cells were gently washed away and any cells that were attached to the surface were stained with a pair of fluorescent dyes (BacLight Live/Dead Bacterial viability kit, Invitrogen, Carlsbad, CA) that stain live cells fluorescent green and dead cells fluorescent red. The position of the adherent live or dead cells on the surface of the slide was then analyzed using an iCyte optical laser scanning cytometer. The iCyte is a modified inverted microscope that scans the surface of the slide and captures an image of each microscopic field using up to 4 fluorescence detectors. The output of each detector was saved and composite images were generated. Fig. 6 shows the results of a mosaic image made from over 500 individual images of a typical gradient slide. The image (Fig. 6a) clearly showed areas where there were very few cells attached, areas where there were large numbers of attached live cells (green), areas where there were large numbers of both live and dead cells (yellow), and areas where there were large numbers of dead cells (red).

The anionic cell membranes were strongly attracted to the cationically charged surface only when the charge density was enough to bind the cells. A solvent accessible surface charge density of less than 1×10^{15} accessible

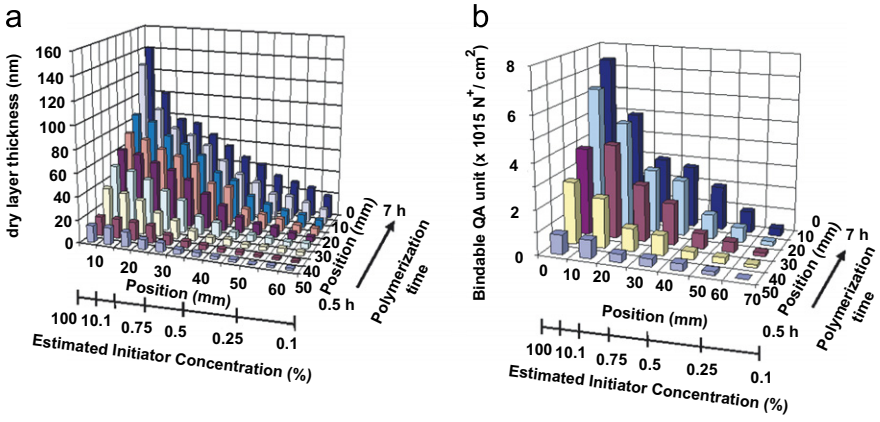

Fig. 5. Dry layer thickness (a) and solvent accessible surface charge density (b) on a combinatorial silicon wafer. Note that the initiator gradient is logarithmic while the time gradient is linear.

Please cite this article as: Murata H, et al. Permanent, non-leaching antibacterial surfaces—2: How high density cationic surfaces kill bacterial.... Biomaterials (2007), doi:10.1016/j.biomaterials.2007.06.012

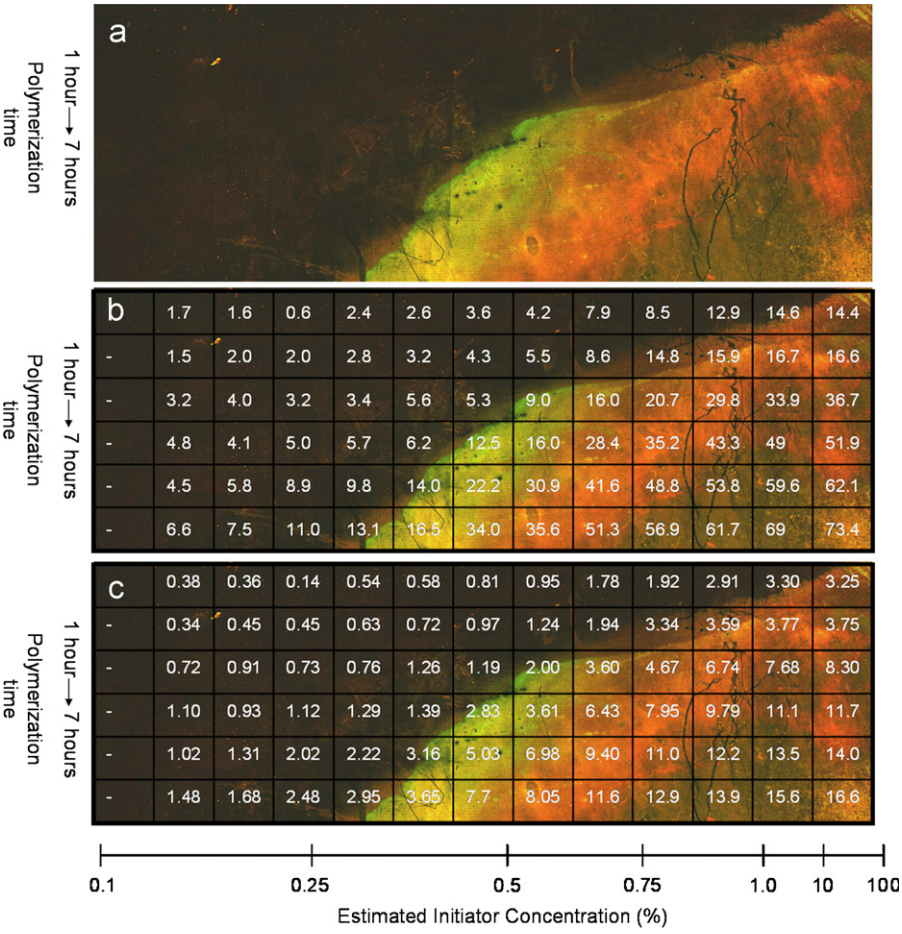

Fig. 6. Mosaic image of a scanned gradient slide. A glass slide co-synthesized with the silicon wafer slide measured in Fig. 6 was tested for its ability to kill *E. coli*: (a) the color image of the slide; (b) the slide with superimposed the layer thickness (nm) data from the co-synthesized silicon wafer; (c) charge density, in positive charges/cm^2 ($\times 10^{15}$), was measured by fluorescein staining of a co-synthesized silicon wafer and the data superimposed.

surface charge/cm^2 was apparently not sufficient to anchor cells in this assay. Moving from the left to the right side of the slide, cells bound more effectively, but the surface did not kill all of them (the dominant color in this region is green). Interestingly, when the fluorescein-staining data was superimposed on the image we observed that a solvent accessible surface charge density of approximately $2–3 \times 10^{15}$ charge/cm^2 was enough to bind cells but not immediately kill them in this assay system. Once the surface charge density exceeded 3×10^{15} charge/cm^2, all cells exposed to that surface were killed within the short time of the exposure regardless of the density and chain length of the surface-linked PQAs at that location. High-density brushes (far right of the slide) were effective biocides whether dry layer thickness was 15 or 75 nm. This combinatorial approach in gradient surface synthesis and the unique iCyte screening tool could be used to optimize kill efficacy with different bacterial species, fungi, human cells, and perhaps even viruses.

To begin to quantify the data from the scanning cytometer and further define the high kill regions, the images were converted into a 3-D plot of intensity data from the red detector (Fig. 7). The apparently black area

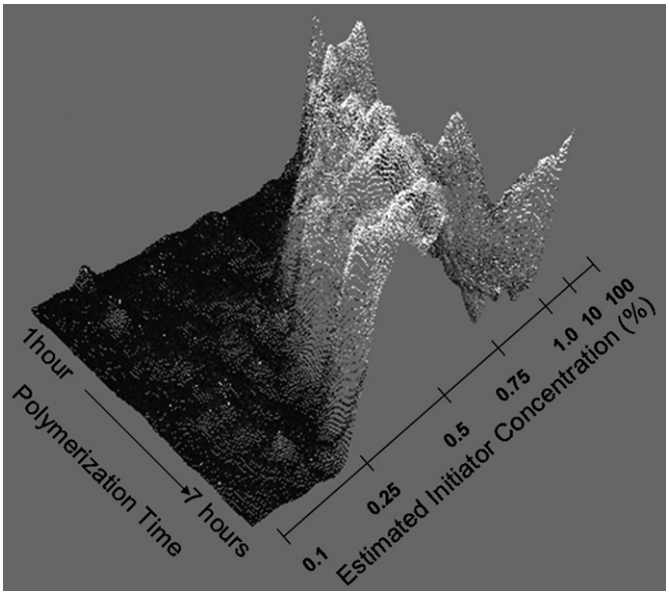

Fig. 7. Surface plot of red pixel density. The density of red pixels is plotted from the digital image of the slide used to generate the pictures in Fig. 7. The polymerization time is a smooth gradient from 1 to 7 h whereas the initiator concentration is a logarithmic gradient from 0.1% to 100% initiator.

Please cite this article as: Murata H, et al. Permanent, non-leaching antibacterial surfaces—2: How high density cationic surfaces kill bacterial.... Biomaterials (2007), doi:10.1016/j.biomaterials.2007.06.012

on the slide was a region where cells did not bind tightly. When the data from the red detector alone is plotted, however, it can be seen that there is some fluorescence in this region showing that there is a small level of kill in this region. This is consistent with the small amount of kill seen for the low-density surfaces described in Tables 1 and 2.

4. Conclusions

The molecular weight dependent cell membrane insertion mechanism has driven the design of a remarkable series of biocidal PQA surfaces since the approach was popularized by the pioneering work of the Klibanov group [1,3,5,6,9,10,12,37]. Our observation that another mechanism dominates the activity of *high density* PQA brushes synthesized by ATRP could drive the development of a new class of surfaces where the focus is on maximizing surface charge rather than chain length. The question of whether surface-linked PQA's kill bacteria by membrane penetration and/or counterion exchange is important. We have shown that fine tuning of surface chemistry leads to high density brush surfaces that cannot kill by cell penetration. Naturally, this does not invalidate any other mechanism. Low-density brushes that are generated when grafting long chain polymers to surfaces may kill cells as described previously. It is also possible that the only way to generate high surface charge on low graft density surfaces is to use very long chains. Further investigation would be needed to elucidate the roles of each mechanism. We now believe that if a cationic surface has greater than 5×10^{15} charges/cm^2, the surface will be able to kill at least a monolayer of *E. coli* cells before becoming susceptible to fouling and reduced bioactivity. It is interesting to note that measurements of the *E. coli* surface charge [43], when converted to number of charges/cm^2, are between 5×10^{14} and 5×10^{15}/cm^2 depending on the growth stage of the cells. This convergence of numbers between the charge density of the cell surface and the charge density of an effective killing surface may be significant and is currently under investigation.

Acknowledgments

This work was supported by Award # HR0011-05-C-0002 from DARPA to AJR. We would like to acknowledge the editorial support of Jon Kilner, MS, MA in restructuring early versions of this manuscript.

Appendix A. Supplementary material

Supplementary data associated with this article can be found in the online version at doi:10.1016/j.biomaterials.2007.06.012.

References

[1] Tiller JC, Liao C-J, Lewis K, Klibanov AM. Designing surface that kill bacteria on contact. Proc Natl Acad Sci USA 2001;98:5981–5.
[2] Kügler R, Bouloussa O, Rondelez F. Evidence of a charge-density threshold for optimum efficiency of biocidal cationic surfaces. Microbiology 2005;151:1341–8.
[3] Milović NM, Wang J, Lewis K, Klibanov AM. Immobilized *N*-alkylated polyethylenimine avidly kills bacteria by rupturing cell membranes with no resistance developed. Biotechnol Bioeng 2005;90:715–22.
[4] Lee SB, Koepsel RR, Morley SW, Matyjaszewski K, Sun Y, Russell AJ. Permanent, nonleaching antibacterial surfaces. 1. Synthesis by atom transfer radical polymerization. Biomacromolecules 2004;5:877–82.
[5] Tiller JC, Lee SB, Lewis K, Klibanov AM. Polymer surfaces derivatized with poly(vinyl-*N*-hexylpyridinium) kill airborne and waterborne bacteria. Biotechnol Bioeng 2002;79:465–71.
[6] Lin J, Tiller JC, Lee SB, Lewis K, Klibanov AM. Insights into bactericidal action of surface-attached poly(vinyl-*N*-hexylpyridinium) chains. Biotechnol Lett 2002;24:801–5.
[7] Cen L, Neoh KG, Kang ET. Surface functionalization technique for conferring antibacterial properties to polymeric and cellulosic surfaces. Langmuir 2003;19:10295–303.
[8] Hu FX, Neoh KG, Cen L, Kang ET. Antibacterial and antifungal efficacy of surface functionalized polymeric beads in repeated applications. Biotech Bioeng 2005;89:474–84.
[9] Lin J, Qui S, Lewis K, Klibanov AM. Bactericidal properties of flat surfaces and nanoparticles derivatized with alkylated polyethylenimines. Biotechnol Prog 2002;18:1082–6.
[10] Lin J, Qiu S, Lewis K, Klibanov AM. On the mechanism of bactericidal and fungicidal activities of textiles covalently modified with alkylated polyethylenimine. Biotechnol Bioeng 2003;83:168–72.
[11] Thome J, Hollander A, Jaeger W, Trick I, Oehr C. Ultrathin antibacterial polyammonium coatings on polymer surfaces. Surf Coat Tech 2003;174–175:584–7.
[12] Lin J, Murthy SK, Olsen BD, Gleason KK, Klibanov AM. Making thin polymeric materials, including fabrics, microbicidal and also water-repellent. Biotechnol Lett 2003;25:1661–5.
[13] Ignatova M, Voccia S, Gilbert B, Markova N, Mercuri PS, Galleni M, et al. Synthesis of copolymer brushes endowed with adhesion to stainless steel surfaces and antibacterial properties by controlled nitroxide-mediated radical polymerization. Langmuir 2004;20:10718–26.
[14] Ikeda T, Hirayama H, Yamaguchi H, Tazuke S, Watanabe M. Polycationic biocides with pendant active groups: molecular weight dependence of antibacterial activity. Antimicrob Agents Chemother 1986;30:132–6.
[15] Ikeda T, Yamaguchi H, Tazuke S. New polymeric biocides: synthesis and antibacterial activities of polycations with pendant biguanide groups. Antimicrob Agents Chemother 1984;26:139–44.
[16] Gilbert P, Moore LE. Cationic anitsepsis: diversity of action under a common epithet. J Appl Micro 2005;99:703–15.
[17] Lenoir S, Pagnoulle C, Detrembleur C, Galleni M, Jerome R. New antibacterial cationic surfactants prepared by atom transfer radical polymerization. J Polym Sci A: Polym Chem 2006;44:1214–24.
[18] Cheng Z, Zhu X, Shi ZL, Neoh KG, Kang ET. Polymer microspheres with permanent antibacterial surface from surface-initiated atom transfer radical polymerization. Ind Eng Chem Res 2005;44:7098–104.
[19] Isquith AJ, Abbott EA, Walters PA. Surface-bonded antimicrobial activity of an organosilicon quaternary ammonium chloride. Appl Microbiol 1972;24:859–63.
[20] Matias V, Beveridge T. Cryo-electron microscopy reveals native polymeric cell wall structure in *Bacillus subtilis* 168 and the existence of a periplasmic space. Mol Microbiol 2005;56:240–51.
[21] Matias VR, Al-Amoudi A, Dubochet J, Beveridge TJ. Cryo-transmission electron microscopy of frozen-hydrated sections of *Escherichia coli* and *Pseudomonas aeruginosa*. J Bacteriol 2003;185:6112–8.
[22] Meroueh SO, Bencze KZ, Hesek D, Lee M, Fisher JF, Stemmler TL, et al. Three-dimensional structure of the bacterial cell wall peptidoglycan. Proc Natl Acad Sci USA 2006;103:4404–9.

[23] Ravikumar T, Murata H, Koepsel RR, Russell AJ. Surface-active antifungal polyquaternary amine. Biomacromolecules 2006;7:2762–9.
[24] Beers KL, Gaynor SG, Matyjaszewski K, Sheiko SS, Moeller M. The synthesis of densely grafted copolymers by atom transfer radical polymerization. Macromolecules 1998;31:9413–5.
[25] Matyjaszewski K, Miller PJ, Shukla N, Immaraporn B, Gelman A, Luokala BB, et al. Polymers at interfaces: using atom transfer radical polymerization in the controlled growth of homopolymers and block copolymers from silicon surfaces in the absence of untethered sacrificial initiator. Macromolecules 1999;32:8716–24.
[26] Pyun J, Matyjaszewski K. Synthesis of nanocomposite organic/inorganic hybrid materials using controlled/"living" radical polymerization. Chem Mater 2001;13:3436–48.
[27] Matyjaszewski K, Xia J. Atom transfer radical polymerization. Chem Rev 2001;101:2921–90.
[28] Pyun J, Kowalewski T, Matyjaszewski K. Controlling polymer chain topology and architecture by ATRP from flat surfaces. Macromol Rapid Commun 2003;24:1043–59.
[29] Zhao B, Brittain WJ. Polymer brushes: surface-immobilized macromolecules. Prog Polym Sci 2000;25:677–710.
[30] Matyjaszewski K, Dong H, Jakubowski W, Pietrasik J, Kusumo A. Grafting from surfaces for "Everyone": ARGET ATRP in the presence of air. Langmuir 2007;23:4528–31.
[31] Braunecker WA, Matyjaszewski K. Controlled/living radical polymerization: Features, developments, and perspectives. Prog Polym Sci 2007;32:93–146.
[32] Ramakrishnan A, Dhamodharan R, Rühe J. Controlled growth of PMMA brushes on silicon surfaces at room temperature. Macromol Rapid Commun 2002;23:612–6.
[33] Kim JB, Bruening ML, Baker GL. Surface-initiated atom transfer radical polymerization on gold at ambient temperature. J Am Chem Soc 2000;122:7616–7.
[34] Jones DM, Brown AA, Huck WTS. Surface-initiated polymerizations in aqueous media: effect of initiator density. Langmuir 2002;18:1265–9.
[35] Huang X, Wirt MJ. Surface initiation of radical polymerization for growth of tethered chains of low polydispersity. Macromolecules 1999;32:1694–6.
[36] Ledbetter Jr JW, Bowen JR. Spectrophotometric determination of the critical micelle concentration of some alkyldimethylbenzylammonium chlorides using fluorescein. Anal Chem 1969;41:1345–7.
[37] Park D, Wang J, Klibanov AM. One-step painting-like coating procedures to make surfaces highly and permanently bactericidal. Biotechnol Prog 2006;22:584–9.
[38] Bhat RR, Tomlinson MR, Genzer J. Orthogonal surface-grafted polymer gradients: a versatile combinatorial platform. J Polym Sci B 2005;43:3384–94.
[39] Shar RR, Merreyes D, Husemann M, Rees I, Abbott NL, Hawker CJ, et al. Using atom transfer radical polymerization to amplify monolayers of initiators patterned by microcontact printing into polymer brushes for pattern transfer. Macromolecules 2000;33:597–605.
[40] Yamamoto S, Ejaz M, Tsujii Y, Fukuda T. Surface interaction forces of well-defined, high-density polymer brushes studied by atomic force microscopy. 2. Effect of graft density. Macromolecules 2000;33:5608–12.
[41] Wu T, Efimenko K, Genzer J. Combinatorial study of the mushroom-to-brush crossover in surface anchored polyacrylamide. J Am Chem Soc 2002;124:9394–5.
[42] Murata H, Koepsel RR, Lee SB, Russell AJ. Biocidal surface agents and methods of synthesizing and evaluating biocidal surface agents. US Patent Application #: 11/601,949.
[43] Walker SL, Hill JE, Redman JA, Elimelech M. Influence of growth phase on adhesion kinetics of *Escherichia coli* D21g. Appl Environ Microbiol 2005;71:3093–9.
[44] E2149-2101. Standard test method for determining the antimicrobial activity of immobilized antimicrobial agents under dynamic contact conditions. In: Annual Book of ASTM Standard 2002. International, A. Ed., West Conshohocken, PA, 2002. 1597p.

Please cite this article as: Murata H, et al. Permanent, non-leaching antibacterial surfaces—2: How high density cationic surfaces kill bacterial.... Biomaterials (2007), doi:10.1016/j.biomaterials.2007.06.012